Dynamical constraints on and signals of phase transition

Klaus Morawetz

Institute of Physics, Technical University Chemnitz, 09107 Chemnitz, Germany
Max-Planck-Institut für Physik komplexer Systeme, Nöthnitzer Straße 38, 01187 Dresden

Nonlocal extension of BUU [1,2]

From real-time Green's functions

$$\frac{\partial f_1}{\partial t}+\frac{\partial \varepsilon_1}{\partial k}\frac{\partial f_1}{\partial r}-\frac{\partial \varepsilon_1}{\partial r}\frac{\partial f_1}{\partial k}=\int \frac{dpdq}{(2\pi)^5}|\mathbf{T}|^2\,\delta\left(\varepsilon_1+\varepsilon_2^- -\varepsilon_3^- -\varepsilon_4^- -2\Delta_E\right)$$
$$\times\left[(1-f_1)(1-f_2^-)f_3^-f_4^- - f_1f_2^-(1-f_3^-)(1-f_4^-)\right]$$

$$f_1 \equiv f(k,r,t) \qquad f_2^- \equiv f(p,r-\Delta_2,t)$$
$$f_3^- \equiv f(k-q-\Delta_K,r-\Delta_3,t-\Delta_t) \qquad f_4^- \equiv f(p+q-\Delta_K,r-\Delta_4,t-\Delta_t)$$

Nonlocal shifts as derivatives of phaseshift given by T-matrix

Nonlocal shifts with realistic potentials [3]

The shifts correspond to classical parameter

$$\Delta_\phi = \alpha|\cos\frac{\theta}{2}|\frac{\vec\kappa+\vec\kappa_f}{|\vec\kappa+\vec\kappa_f|}$$
$$\Delta_{\rm HS} = 2d|\sin\frac{\theta}{2}|\frac{\vec\kappa-\vec\kappa_f}{|\vec\kappa-\vec\kappa_f|}$$
$$\Delta_f = \Delta_t\frac{\vec K}{m_a+m_b}$$

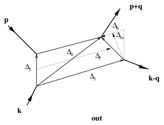

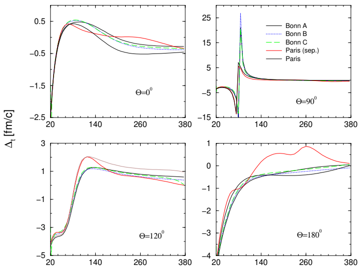

The time delay versus lab energies for different scattering angles.

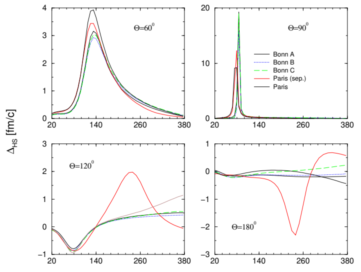

The Enskog displacement parameter d versus lab energies.

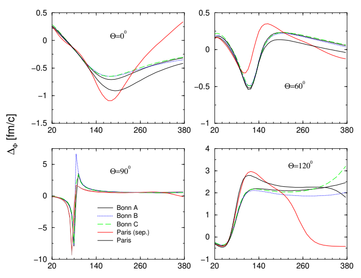

The molecule rotation displacement α versus lab energies.

Comparison with experimental data

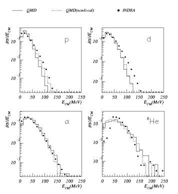

Energy spectra of particles for central $^{129}Xe \to {}^{119}Sn$ [4]

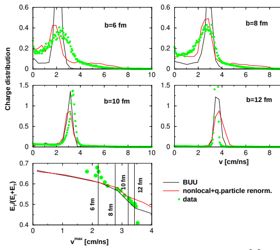

The experimental charge distribution $Ta+Au$ at 33 MeV [5] versus velocity in comparison with in the BUU and the nonlocal model with quasiparticle renormalizations. The maximum velocity versus ratio of longitudinal to total kinetic energy determines the selected experimental cuts.

Nonequilibrium Thermodynamics [6]

From distribution function local quantities (densities)

$$\begin{array}{ll} \text{number} & n(\mathbf{r},t)\\ \text{current} & \mathbf{J}(\mathbf{r},t)\\ \text{kin. energy} & E_K(\mathbf{r},t)\end{array} = \sum_p \begin{pmatrix}1\\ \mathbf{p}\\ \frac{p^2}{2m}\end{pmatrix} f(\mathbf{p},\mathbf{r},t)$$

Global variables/particle by spatial integration

kin. energy $E_K(t) = \int d\mathbf{r} E_K(\mathbf{r},t)$

Fermi energy $E_F(t) = \int d\mathbf{r} E_f[n(\mathbf{r},t)]n(\mathbf{r},t) \Big/ \int d\mathbf{r} n(\mathbf{r},t)$

coll. energy $E_{\rm coll}(t) = \int d\mathbf{r} \frac{J(\mathbf{r},t)^2}{mn(\mathbf{r},t)} \Big/ \int d\mathbf{r} n(\mathbf{r},t)$

Meanfield $U(t) = \int d\mathbf{r}\left(\frac{an^2}{2n_0}+\frac{bn^{s+1}}{(s+1)n_0^s}\right) \Big/ \int d\mathbf{r} n(\mathbf{r},t)$

Bin. corr energy $E_2(t) = E_F^2\frac{2Ln2-11}{70\pi^3}\frac{m}{\hbar^2}\sigma + o(T^3)$

Temperature-independent plots

Fermi liquid temperature $E_K(t) = \frac{3}{5}E_F(t)+E_{\rm coll}(t)+\frac{\pi^2}{4E_F(t)}T(t)^2$

Pressure/particle

$$P = \frac{2}{3}(E_K(t)-E_{\rm coll}(t))+\frac{4}{3}E_2(t)+\int d\mathbf{r}\left(\frac{an}{2n_0}+\frac{bsn^s}{(s+1)n_0^s}\right)\Big/\int d\mathbf{r} n(\mathbf{r},t)$$

"Energy" : $E(t) = E_K(t)-E_{\rm coll}(t)+U(t)$

Equilibrium spinodal:

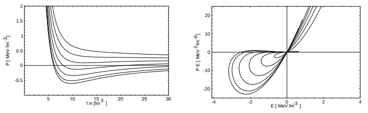

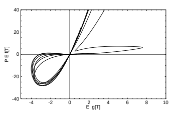

temperature independent plot iso -nothing

Dynamical trajectories

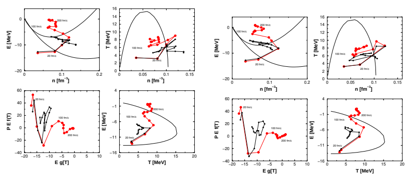

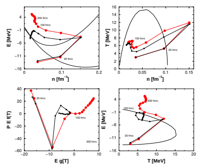

Dynamical trajectories in nonlocal and local BUU (black) scenario for ^{129}Xe on ^{119}Sn at $25, 33, 50$MeV lab energy (from left to right), times steps of 20fm/c up to 300fm/c, zero temperature mean field energy (thick line) and the pressure (thin line) in upper left picture, spinodal line for infinite matter in right figures, scaled temperature-independent plot in left lower plane

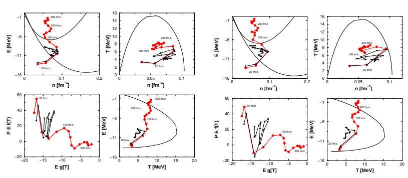

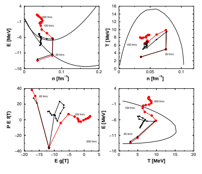

The same dynamical trajectories but for a reaction ^{56}Ni on ^{179}Au at $25, 33, 50$MeV lab energy.

Summary and Prediction

- Nonlocal kinetic theory leads to different nonequilibrium thermodynamics compared to BUU
- Two mechanisms of instability, exp.: [7] and TAPS [8] simulation results here: surface compression and spinodal decomposition
- Predictions for current reactions:

E[MeV]	25	33	50
$^{58}_{28}$Ni + $^{197}_{79}$Au	S	C S	C (S)
$^{129}_{54}$Xe + $^{119}_{50}$Sn	C S	C (S)	C

E[MeV]	15	33	60
$^{157}_{64}$Gd + $^{238}_{92}$U	–	C S	C
$^{181}_{73}$Ta + $^{197}_{79}$Au	C S	C (S)	C

- Fast surface eruption happens outside spinodal region
- For higher energies there is not enough time to rest at the spinodal, system decays before
- Prediction nicely confirmed by Δ-scaling of INDRA data [9]
- Nonlocal extension of BUU describes enhancement of high energetic spectra of protons and the midrapidity charge distribution better
- Flow calculations by nonlocal BUU in better agreement with data (under preparation)

References

[1] P. Lipavský, K. Morawetz, and V. Špička, *Kinetic equation for strongly interacting dense Fermi systems*, Vol. 26,1 of *Annales de Physique* (EDP Sciences, Paris, 2001), .

[2] K. Morawetz, P. Lipavský, and V. Špička, Ann. of Phys. **294**, 134 (2001).

[3] K. Morawetz, P. Lipavský, V. Špička, and N.-H. Kwong, Phys. Rev. C **59**, 3052 (1999).

[4] K. Morawetz *et al.*, Phys. Rev. Lett. **82**, 3767 (1999).

[5] K. Morawetz *et al.*, Phys. Rev. C **63**, 034619 (2001).

[6] K. Morawetz, Phys. Rev. C **62**, 44606 (2000).

[7] H. Ngo *et al.*, in *Proceedings of the international workshop* (GSI, Hirschegg, Kleinwalsertal, 1993), p. 302.

[8] Y. Schutz and et. al., Nucl. Phys. A **622**, 404 (1997).

[9] R. Botet *et al.*, Phys. Rev. Let. **86**, 3514 (2001).